Clim. Past Discuss., 8, 1687–1720, 2012
www.clim-past-discuss.net/8/1687/2012/
doi:10.5194/cpd-8-1687-2012

Climate of the Past Discussions

Bunker Cave stalagmites: an archive for central European Holocene climate variability

J. Fohlmeister[1], A. Schröder-Ritzrau[1], D. Scholz[2], C. Spötl[3], D. F. C. Riechelmann[4], M. Mudelsee[5], A. Wackerbarth[1], A. Gerdes[6,7], S. Riechelmann[8], A. Immenhauser[8], D. K. Richter[8], and A. Mangini[1]

[1]Heidelberg Academy of Sciences, Heidelberg, Germany
[2]Institute for Geosciences, University of Mainz, Mainz, Germany
[3]Institute for Geology and Palaeontology, University of Innsbruck, Innsbruck, Austria
[4]Institute for Geography, University of Mainz, Mainz, Germany
[5]Climate Risk Analysis, Hanover, Germany
[6]Institute for Geosciences, Goethe University Frankfurt, Frankfurt, Germany
[7]Department of Earth Sciences, Stellenbosch University, Private Bag X1, Matieland 7602, South Africa
[8]Institute for Geology, Mineralogy and Geophysics, Ruhr-University Bochum, Bochum, Germany

Received: 29 March 2012 – Accepted: 29 April 2012 – Published: 11 May 2012

Correspondence to: J. Fohlmeister (jens.fohlmeister@iup.uni-heidelberg.de)

Published by Copernicus Publications on behalf of the European Geosciences Union.

Abstract

Holocene climate was characterised by variability on multi-centennial to multi-decadal time scales. In central Europe, these fluctuations were most pronounced during winter. Here we present a new record of past winter climate variability for the last 10.8 ka based on four speleothems from Bunker Cave, Western Germany. Due to its central European location, the cave site is particularly well suited to record changes in precipitation and temperature in response to changes in the North Atlantic realm. We present high resolution records of $\delta^{18}O$, $\delta^{13}C$ values and Mg/Ca ratios. We attribute changes in the Mg/Ca ratio to variations in the meteoric precipitation. The stable C isotope composition of the speleothems most likely reflects changes in vegetation and precipitation and variations in the $\delta^{18}O$ signal are interpreted as variations in meteoric precipitation and temperature. We found cold and dry periods between 9 and 7 ka, 6.5 and 5.5 ka, 4 and 3 ka as well as between 0.7 to 0.2 ka. The proxy signals in our stalagmites compare well with other isotope records and, thus, seem representative for central European Holocene climate variability. The prominent 8.2 ka event and the Little Ice Age cold events are both recorded in the Bunker cave record. However, these events show a contrasting relationship between climate and $\delta^{18}O$, which is explained by different causes underlying the two climate anomalies. Whereas the Little Ice Age is attributed to a pronounced negative phase of the North Atlantic Oscillation, the 8.2 ka event was triggered by cooler conditions in the North Atlantic due to a slowdown of the Thermohaline Circulation.

1 Introduction

The Holocene represents an epoch of relatively stable, warm climate conditions, in particular in comparison to the large, rapid changes that occurred during the Last Glacial. The largest climate anomaly during the Holocene was the short 8.2 ka cold event (Alley et al., 1997), which has been identified in several climate records (e.g. von Grafenstein

CPD
8, 1687–1720, 2012

et al., 1998; North Greenland Ice Core Project members, 2004; Boch et al., 2009). However, for Europe, several periods during the Holocene with warm/wet and cold/dry climate, respectively, have been reported (see, for instance, the summaries in Wanner et al., 2008, 2011).

Various archives for terrestrial past climate variability have been evaluated in order to disentangle the complex patterns of Holocene climate change. For instance, numerous studies on tree rings (e.g. Friedrich et al., 1999; Spurk et al., 2002; Büntgen et al., 2010), lake sediments (e.g. Guiot et al., 1993; Magny, 2004; Davis et al., 2003, and references therein) and glaciers (e.g. Holzhauser et al., 2005; Joerin et al., 2006; Ivy-Ochs et al., 2009) contributed important information on past Holocene climate variability in Europe. Most of these archives are known to mainly record spring to summer conditions. In contrast, speleothems, and stalagmites in particular, provide the opportunity to reconstruct climate conditions during autumn and winter in central Europe (Wackerbarth et al., 2010). The main reason for this is that enhanced evapo-transpiration during spring and summer months leads to reduced infiltration into the karst aquifer. Thus, the major proportion of the drip water feeding the speleothems in most Central European caves originates from winter precipitation. In order to gain comprehensive insight into past climate variability it is important to differentiate between different seasons. For example, Davis et al. (2003) showed in a compilation of European pollen data that temperature variations during the Holocene largely differ between the warm and cold seasons, with larger fluctuations occurring during winter.

Within the last decade, several Holocene climate reconstructions for central Europe based on speleothems have been published (e.g. McDermott et al., 1999; Frisia et al., 2003; Niggemann et al., 2003; Mangini et al., 2005; Vollweiler et al., 2006; Boch et al., 2009). However, none of the currently available speleothem records for Central Europe covers the entire Holocene. Here we present a Central European composite stalagmite record from Bunker Cave, Western Germany, covering the last 10.8 ka. We show high-resolution stable C and O isotope data as well as Mg/Ca ratios. This

CPD
8, 1687–1720, 2012

multi-proxy reconstruction enables a robust reconstruction of past winter climate variability in Central Europe.

2 Cave site and methods

2.1 Cave site description

Bunker cave is located at 51°22′03″ N, 7°39′53″ E in Western Germany (Sauerland, Fig. 1) and belongs to a large cave system, which consists of several closely situated caves. Bunker Cave was discovered in 1926 during road works, and during the Second World War the entrance area of the cave was artificially enlarged. The entrance to the cave is situated 184 m a.s.l. on a south-facing hill slope. The cave is developed in Middle to Upper Devonian, low-Mg limestone hosting thin dolomite veins. The thickness of the host rock above the cave ranges from 15 to 30 m, which is covered by up to 70 cm of soil (inceptisol/alfisol developed from loess loam). Vegetation above the cave consists entirely of C3 plants, i.e. mainly ash and beech as well as scrub vegetation. The mean annual air temperature in the cave is about 10.8 °C, and the mean annual amount of precipitation in the area is around 950 mm yr^{-1}. Further details can be found elsewhere (e.g. Immenhauser et al., 2010; Kluge et al., 2010; Riechelmann, et al., 2011; Münsterer et al., 2012).

Four speleothems, which grew within a maximum distance of 12 m from each other, were removed from the cave for this study (Bu1, Bu2, Bu4 and Bu6). Stalagmite Bu1 has a length of about 65 cm. Bu2 and Bu4 are approximately 20 cm long, whereas Bu6 is a flowstone with a length of about 6 cm (Fig. 1). All stalagmites have a diameter of about 5 to 10 cm and were sampled under actively dripping sites. The drip sites of the investigated stalagmites have been monitored within the framework of a comprehensive, long-term cave monitoring program Riechelmann, et al. (2011). The $\delta^{18}O$ values of the drip water show that the recharge water is well mixed within the aquifer

CPD
8, 1687–1720, 2012

and corresponds to the infiltration weighted annual mean $\delta^{18}O$ value of precipitation (Wackerbarth et al., 2010; Riechelmann, et al., 2011).

2.2 Methods

2.2.1 Th/U dating

Samples for Th/U-dating were cut from the growth axis of the stalagmites using a diamond-coated band saw. The thickness (in growth direction) of individual samples is typically 4 mm. All samples were analysed by thermal ionisation mass spectrometry (TIMS) at the Heidelberg Academy of Sciences. Methods used for sample preparation and mass spectrometric analysis are explained in detail in Frank et al. (2000) and Holzkämper et al. (2005). The calibration of the U and Th spikes is described in Hoffmann et al. (2007). Due to the relatively low U content of the samples Th/U-dating of Holocene speleothems from Bunker Cave using the TIMS method is challenging. Therefore, a Th solution with precisely determined concentration and isotopic composition was added to some sub-samples in order to increase the analysis time for Th and to improve counting statistics. The measured isotope ratios were corrected accordingly and the uncertainties in concentration and isotope composition of the added Th solution were propagated to the final age errors. Ages were calculated using the half lives of Cheng et al. (2000). Correction for detrital contamination assumes a $^{232}Th/^{238}U$ concentration ratio of 3.8 ± 1.9 and ^{230}Th, ^{234}U and ^{238}U in secular equilibrium. Age uncertainties are quoted at the 2-σ level and do not include half-life uncertainties. The reference year for all ages given in the study is AD 1950.

2.2.2 Radiocarbon dating

Samples for radiocarbon dating were drilled in a CO_2-free atmosphere in the Heidelberg radiocarbon laboratory using a hand-held dental drill with a burr diameter of 1 mm. Sub-samples from the very top of the stalagmites were milled from the stalagmite

CPD
8, 1687–1720, 2012

surface. The uppermost layers (~100 µm) of the stalagmite, which may be contaminated due to exchange with atmospheric carbon, were not used for analysis. The $CaCO_3$ powder was acidified (HCl) in vacuo, and the resulting CO_2 was combusted with H_2 to C on a Fe catalyst at 575 °C. The samples were measured at the MICADAS at ETH Zurich (Synal et al., 2007).

2.2.3 Stable isotopes

The stalagmites were micromilled continuously along the growth axis at increments of 0.3 mm for Bu1 and Bu6, 0.2 mm for Bu4 and 0.15 mm for Bu2. Stable C and O isotopes were measured at the triple collector gas source isotope ratio mass spectrometer of the University of Innsbruck. The mass spectrometer is linked to an on-line, automated carbonate preparation system (for details, see Spötl and Mattey, 2006). Isotope ratios are reported against the VPDB scale and the 1σ precision is 0.06 and 0.08 ‰ for $\delta^{13}C$ and $\delta^{18}O$, respectively.

2.2.4 Mg and Ca analyses

The stalagmites were cut along the growth axis into 2 cm-long pieces, which were mounted in epoxy resin discs and polished. Mg/Ca ratios were measured parallel to the growth axis. The continuous profile is located within 2 mm of the stable isotope track. Mg/Ca ratios of the speleothems were measured by Laser Ablation ICP-MS (LA-ICPMS) at the Mineralogical Institute, Frankfurt, Germany, using a New Wave UP213 ultraviolet laser system, coupled to a Themo-Finnigan Element II sector field ICP-MS (Gerdes and Zeh, 2006). Element data were continuously acquired using a 60 µm circular ablation spot and a scan speed of 10 $\mu m\,s^{-1}$. The method produces approximately 40 data points per mm corresponding to a spatial resolution of 25 µm. Background counts, measured with the laser in off mode, were subtracted from the raw data. All data are normalized to the Ca content of the calcite and standardized against NIST

CPD
8, 1687–1720, 2012

612 glass (Pearce et al., 1996), which was measured before and after each sample. A continuous sample scan had a maximum length of 2 cm.

2.2.5 Microscopy

Thin sections were made from all four stalagmites by sawing a thin slice near the growth axis, next to the element track, which were broken into approximately 4 cm long pieces in order to obtain a continuous series of thin sections. These pieces were stuck on small glass plates and polished to 30 µm thickness. These thin sections were examined using standard transmitted-light microscopy as well as using a hot cathode-CL-microscope (type Lumic HC1-LM; Neuser et al., 1995).

3 Results

3.1 Th/U-dating and microscopic analysis

Ten sub-samples from stalagmite Bu1, four sub-samples from Bu2, eleven sub-samples from Bu4 and three sub-samples from Bu6 were dated (Table 1). Dating of the samples was challenging due to the relatively low U content (~ 0.1 ppm). The 2σ-age uncertainty is between 100 and 300 a for most samples (Table 1). Some samples contain elevated amounts of detritial Th (between 2 and 3 ng g^{-1}, Table 1) leading to significant age corrections. Stalagmite Bu6 covers the period between 10.7 and 8.8 ka BP, and the Holocene part of Bu2 (i.e. ~ the upper 7 cm) grew between 10.7 and 7.7 ka BP. Bu4 covers the last approximately 8.1 ka (Fig. 2). Thin sections revealed that Bu4 is dominated by columnar crystals, which indicates relatively slow and constant growth rates. Two small detritus layers were observed at about 15 and 17 cm distance from top (dft), which are identified as coralloid layers (Fig. 3b). These layers probably reflect periods of limited growth, which, however, seem to have been short since Th/U dating does not resolve a growth stop. Petrographic investigation of Bu1 shows at approximately 17 cm dft a detritus-rich layer revealing a hiatus. The duration of this interruption

CPD
8, 1687–1720, 2012

of stalagmite growth cannot be determined precisely due to unreliable Th/U dates in the interval between 14.6 and 30 cm dft. Hence, age data for Bu1 are only presented between the top and 14 cm dft as well as from 31 to 49 cm dft including the periods between "pre-modern" (Sect. 3.2) and 1.6 ka BP as well as 4.7 and 6.7 ka BP (Fig. 2). During the latter period Bu1 consists mainly of fast growing dendritic crystals, in agreement with the growth rate derived from the age measurements. In the section below ~ 49 cm dft, it was again impossible to measure reliable dates. The bottom section of Bu1 (~ 10 cm) grew during the Eemian. Thin section analysis of the top of Bu2 and Bu6 indicate brown layers, which are interpreted as detrital layers highlighting hiati. Hence, data for the upper 7 (Bu2) and 2 mm (Bu6) were discarded. The other parts of Bu2 and Bu6 as well as the younger part of Bu1 are solely formed of columnar crystals (Fig. 3b), which reveal relatively slow and constant growth rates.

3.2 Radiocarbon

Three radiocarbon analyses were performed at the top sections of stalagmite Bu4 and Bu1. This enabled to test whether the stalagmites stopped growing before or after the atmospheric radiocarbon anomaly in the middle of the 20th century (e.g. Levin and Kromer, 2004; Hua and Barbetti, 2004). Due to the low U content (Table 1) the Th/U age data are not precise enough to verify/falsify recent speleothem growth. Bu1 does not show a clear bomb-peak, whereas Bu4 reveals a typical increase and decrease in its uppermost 2 mm as expected for the radiocarbon bomb-pulse captured in stalagmites (see e.g. Genty and Massault, 1999; Mattey et al., 2008; Fohlmeister et al., 2011, Table 2). This suggests that Bu4 was actively growing until its removal, whereas Bu1 definitely stopped growing before 1950 AD.

3.3 Chronology

The growth phases of all four stalagmites cover the last 10.8 ka. During several intervals, two stalagmites grew contemporaneously (i.e. from 0 to 1.6 ka; from 4.7 to 6.7 ka;

CPD
8, 1687–1720, 2012

from 7.7 to 8.1 ka and between 8.8 and 10.7 ka, Fig. 2). Thus, it is possible to test whether the proxy signals recorded in individual stalagmites are reproducible. If this is the case, a dominant influence of local, drip-site specific effects can be ruled out, and the proxy signals likely reflect past climate variability. The temporally overlapping sections allow to assemble a composite record. We a priori assume that the O isotope records of the four stalagmites represent one common signal. The records are combined with *iscam* (intra-site correlation age modelling; Fohlmeister, 2012). This method correlates dated proxy signals from several stalagmites, determines the most probable age-depth model and calculates the age uncertainty for the combined record. *Iscam* enables to quantitatively verify whether signals from two individual stalagmites have a common signal within the age errors. Furthermore, the algorithm is able to prove whether the resulting correlation is statistically significant. This provides the advantage of enlarging the signal-to-noise ratio and minimising the age uncertainties within the overlapping periods. In addition, *iscam* allows to prove if the signals of two archives correlate above significance limits, which indicate that the observed variations have a common cause.

For age-depth modelling, both the Th/U ages and the radiocarbon measurements are used. An additional constraint is given by calcite supersaturated drip water from the active drip site. Therefore, we prescribed the top age of Bu4 to be 1997 AD ± 10 yr for the age-depth modelling (Bu4 was removed in 2007 AD). For the top of Bu1, the ^{14}C bomb peak is not visible. Thus, the stalagmite definitely stopped growing before 1950 AD. In addition, the strong increase in $\delta^{13}C$ observed for Bu4 is not present in Bu1 (Sect. 3.4, Fig. 3) suggesting that Bu1 stopped growing before the $\delta^{13}C$ increase. We assume an age of 100 ± 40 a BP for the top section of Bu1.

Iscam uses the available age information (means and errors) and the variation in the $\delta^{18}O$ signal of the four stalagmites in order to obtain the best age-depth model. For a detailed description of the method the reader is referred to the original publication (Fohlmeister, 2012). Usually, the age uncertainties in the overlapping periods are smaller than in the periods without overlaps (Fig. 2). Hence, jumps in the uncertainty

CPD
8, 1687–1720, 2012

range may occur at transitions between overlapping and non-overlapping parts. The shaded areas of the overlapping periods between Bu4 and Bu2 as well as between Bu2 and Bu6 represent 68 % confidence intervals. The correlation coefficient of the according δ^{18}O time series does not exceed the 95 % threshold. The threshold to the 95 % interval for the correlation coefficient between Bu2 and Bu6 is only missed by 0.01. The reason for missing the 95 % interval range between Bu2 and Bu4 is related to the relatively short overlapping interval between both stalagmites (Fohlmeister, 2012).

3.4 C and O isotope and Mg/Ca time-series

Given that the spatial resolution of the Mg/Ca elemental ratios exceeds that of the carbon and oxygen isotope record, the elemental proxy has been brought to the resolution of the δ^{13}C and δ^{18}O records. For this purpose, all Mg/Ca ratios within the depth range of one stable isotope sample have been averaged. The Mg/Ca data (Fig. 3a) show a decreasing trend within the last 10.8 ka. During the early Holocene, Mg/Ca ratios are approximately twice as high as in the recent period, 0.0033 and 0.0015, respectively. Both the absolute Mg/Ca values and the pattern are similar in overlapping parts of Bu2, Bu4 and Bu6 suggesting that all three stalagmites experienced comparable hydrological conditions in agreement with findings from present day cave monitoring. The Mg/Ca ratio of Bu6 is slightly lower than that of Bu2. Stalagmite Bu1 shows significantly lower values than Bu4. Similarly, the Mg/Ca patterns of Bu1 and Bu4 are – apart from the generally decreasing trend – different (Fig. 3a).

The total range of the δ^{13}C values of the four Bunker Cave stalagmites is between −12 and −5 ‰ (Fig. 3c). In the early Holocene, Bu2 and Bu6 show δ^{13}C values between −9 and −10 ‰. As for Mg/Ca, the values of Bu6 are lower than those of Bu2. The δ^{13}C values of Bu2 increase between 8.5 and 7.5 ka, which is in agreement with the Bu4 record. The δ^{13}C values of the four Bunker stalagmites show maximum values about −7 ‰ between 8 and 6 ka. After 6 ka, the δ^{13}C values of Bu4 decrease. In the recent past, Bu4 shows a steep increase by about 4 ‰ in δ^{13}C. Bu1 generally shows the same pattern as Bu4, especially in the young section of the two stalagmites. However,

CPD
8, 1687–1720, 2012

the $\delta^{13}C$ values of Bu1 are lower compared to those of Bu4. Furthermore, the rapid increase measured in the recent part of Bu4 is not visible in Bu1 (Fig. 3c) confirming that Bu1 stopped growing before this anomaly occurred.

The $\delta^{18}O$ values were used to determine the age model for the composite record. Therefore, the $\delta^{18}O$ records in overlapping parts of different stalagmites are in agreement (Fig. 3d). The high correlation coefficients (0.9 for the young parts of Bu1 and Bu4, 0.79 for the old parts of Bu1 and Bu4, 0.72 for Bu2 and Bu4 and 0.76 for Bu2 and Bu6) strongly suggest that the $\delta^{18}O$ values reflect climate conditions above Bunker Cave rather than site specific effects. This is also supported by the similar absolute $\delta^{18}O$ values of all four stalagmites. $\delta^{18}O$ variability during the last 10.8 ka is in the range of 2 ‰, with the highest values observed at 0.5 ka (−5 ‰) and the lowest values (−7 ‰) recorded around 10 ka (Fig. 3d).

4 Discussion

4.1 Mg/Ca ratios

Previous work suggested that the speleothem calcite Mg/Ca ratio is a qualitative proxy for the amount of precipitation above the cave or infiltration into the karst aquifer (see Fairchild and Treble, 2009, and citations therein). However, a sound understanding of the geochemical processes and flow characteristics, which are most likely unique for each cave system, is mandatory for the interpretation of this proxy. Regarding the Mg/Ca records from Bunker Cave, first, an explanation approach for the long-term decreasing trend in the Mg/Ca ratio of the stalagmites Bu2 and Bu4 during the Early to Middle Holocene (Fig. 3a) is required. For this purpose, possible variations of the drip water sources, feeding the stalagmite, must be considered.

Modern rain water at the cave location has a maximum Mg/Ca ratio of 0.2 ± 0.1 (Riechelmann, et al., 2011). Water in the upper soil zone above Bunker Cave has a very low Ca concentration and a Mg/Ca ratio of 0.13 ± 0.01. This is related to weathering

CPD
8, 1687–1720, 2012

of the non-carbonate loam fraction of the soil, such as Mg-bearing chlorite, montmorillonite and illite. Weathering of this siliceous soil material is also documented in seasonal changes in drip water Mg isotope composition (Riechelmann, S. et al., 2012). During percolation through the low Mg Devonian limestone, the water dissolves the host rock with, in average, lower Mg/Ca ratios than the soil water (Mg/Ca: 0.004–0.008, $n = 5$). The resulting drip water feeding the stalagmite represents, thus, a mixture of the Mg/Ca ratios of meteoric precipitation, soil zone clay content and host rock carbonate resulting in a Mg/Ca ratio of the drip water of 0.02–0.06 (Riechelmann, et al., 2011). Towards the end of the Last Glacial period, loess was deposited above Bunker Cave. This loess may have had a higher proportion of weathered late diagenetic dolomite than today, which is sporadically found in the host rock (Hammerschmidt et al., 1995). Weathering and leaching during the transition and the Early Holocene removed some of the Mg bearing loess cover and may have resulted in relatively high Mg/Ca ratios in the stalagmites during the Early Holocene. Progressive weathering and decalcification may have led to elution of the initially high Mg components of the aeolian deposits causing Mg/Ca ratios in the stalagmite to decrease. This may coincide with enhanced weathering in the Atlantic stage as postulated by Richter et al. (2004).

Whereas the long-term trend in Mg/Ca is caused by successive decalcification of the loess cover, short-term variations in Mg/Ca ratios are attributed to the amount of precipitation or infiltration. The extensive long-term monitoring at Bunker Cave (Riechelmann, et al., 2011) reveals that a major process affecting the Mg/Ca ratio in stalagmites is Prior Calcite Precipitation (PCP), e.g. calcite which precipitates before the solution reaches the stalagmite. Lower infiltration into the karst aquifer leads to a higher proportion of air compared to water in the host rock favouring degassing of CO_2 and, thus, PCP. Lower rainfall amounts also lead to lower drip rates and, thus, foster PCP at the cave ceiling. In both cases, the Mg/Ca ratio in the stalagmites should increase as has been demonstrated in various studies (Tooth and Fairchild, 2003; Cruz Jr et al., 2007). The effect of PCP on the Mg/Ca ratio during dry periods is further amplified by an additional process: Longer residence times of the percolating water in the host rock are

CPD
8, 1687–1720, 2012

result in higher Mg/Ca ratios due to the different dissolution characteristics of calcite and dolomite (Fairchild and Treble, 2009).

We interpret the short-term variations in the Mg/Ca ratios of the Bunker cave stalagmites during the Holocene (Fig. 3a) as precipitation variability above the cave. The detrended Mg/Ca ratio (Fig. 4a) is, therefore, interpreted as a proxy for precipitation amount. Higher Mg/Ca ratios in the detrended record are interpreted as dryer periods and vice versa. Based on this interpretation, periods around 0.5, 4.5–3.7, 5.6 and 7.7–7.3 ka BP were characterised by relatively dry conditions. This is supported by the findings of the microscopy analyses. At 5.6 ka a thin coralloid layer was found in Bu4 (Fig. 3b). This kind of calcite fabric is formed from aerosols and can therefore only grow during extrem dry conditions, when there is less drip water available (Hill and Forti, 1997). The period between 7–8 ka in Bu4 is dominated by columnar fabrics indicating dryer conditions (Frisia and Borsato, 2010) and contains a further coralloid layer.

The Mg/Ca ratio of Bu1 and its variability is generally lower than that of Bu4 when comparing coeval time intervals (Fig. 3a). This indicates that Bu1 either experienced a faster drip rate resulting in less PCP or a shorter residence time in the karst aquifer resulting in a lower Mg concentration due to less intensive dolomite dissolution. This interpretation agrees with the observations reported in (Riechelmann, et al., 2011) for monthly collected drip water samples from the drip sites above the two speleothems. The recent drip rate of Bu1 is by about two orders of magnitude faster than the drip rate of Bu4. Furthermore, Mg isotopes showed that the Mg contribution to drip waters is variable showing different Mg proportions derived from the soil and karst, which may explain the Mg/Ca offset between stalagmite Bu1 and Bu4 (Riechelmann, S. et al., 2012).

4.2 δ^{13}C values

Monitoring of Bunker Cave drip water (Riechelmann, et al., 2011) showed only small variability in the δ^{13}C values of annual drip water collected at different drip sites in the

CPD
8, 1687–1720, 2012

cave. Similarly, only small differences in annual cave air pCO_2 and $\delta^{13}C$ were detected. Therefore, we can neither attribute the long-term trend nor the short-term variations in speleothem $\delta^{13}C$ values (Fig. 3c) to changes in the seasonality of calcite precipitation or cave ventilation as has been demonstrated for other caves (e.g. Spötl et al., 2005; Frisia et al., 2011; Tremaine et al., 2011). The large increase in the $\delta^{13}C$ values of Bu4 in the last 250 a (Fig. 3c) is anomalous and may be related to the artificial opening of the cave in the late 19th to early 20th century. The $\delta^{13}C$ values of the top section of Bu4 agree well with the $\delta^{13}C$ values of recent calcite precipitates from this drip site (Riechelmann, D. F. C. et al., 2012).

The $\delta^{13}C$ values of Bu1 are lower than those of Bu4 during joint growth periods. The mean offset between both records is ca. 1.3 ‰. This offset may partly reflect differences in the $\delta^{13}C$ value of the drip water. Modern drip water $\delta^{13}C$ values differ by approximately 0.13 ‰ (Riechelmann, D. F. C. et al., 2012). In addition, variable kinetic isotope fractionation due to different drip rates may have affected the two speleothems, which would further increase the difference in $\delta^{13}C$ values (Scholz et al., 2009; Dreybrodt and Scholz, 2011). Today, the drip rate of Bu1 is about two orders of magnitude faster than that of Bu4, which is consistent with the interpretation of the calcite $\delta^{13}C$ values of Bu1 and Bu4.

A similar assessment for the observed differences in stalagmite $\delta^{13}C$ values is also possible using the measured ^{14}C values (Table 2). Since monitoring data suggest that the drip water of both drip sites originates from the same soil water reservoir, the initial soil water $\delta^{13}C$ and ^{14}C values should be comparable for both drip sites. Thus, the observed variability in the drip water should be related to the process of carbonate dissolution, such as the degree of open versus closed conditions, respectively, as well as potential differences in PCP and kinetic isotope fractionation. Bu1 has a dead carbon fraction (dcf) of approximately 7 %, whereas Bu4 has a dcf of about 12 % (Table 2). According to similar calculations as described in Griffiths et al. (2012) and assuming mean soil air $\delta^{13}C$ values of about −23 ‰, host rock $\delta^{13}C$ values of +3.5 ‰ (Wurth, 2002) and a mean temperature of 10 °C, the $\delta^{13}C$ values of the Ca-saturated water

CPD
8, 1687–1720, 2012

feeding Bu1 should be about 0.5 to 0.6 ‰ lower than that feeding Bu4. The remaining 0.7 to 0.8 ‰ are attributed to PCP and kinetic isotope fractionation effects. This is consistent with the observed lower modern drip rates feeding Bu4 and the offset in the Mg/Ca ratio of the two stalagmites.

The increase in the δ^{13}C values of about 3 ‰ during the early Holocene and the subsequent decrease (Fig. 3c) may have been caused by several effects. Higher δ^{13}C values may originate by increased kinetic isotope fractionation on the stalagmite (Scholz et al., 2009; Mühlinghaus et al., 2009) or even on the stalactite (Frisia et al., 2011) as well as by a larger contribution of host rock-derived C and/or by lower root respiration and soil microbial activity resulting in more positive soil gas δ^{13}C values (Cerling, 1984). Although it is difficult to identify which of these processes dominated the long-term trend in the δ^{13}C values of the stalagmite record, we hypothesise that more positive soil air δ^{13}C values modulated by vegetation density was the major influence. This assumption is based on the relatively slow adjustment of vegetation compared to the faster reaction time of carbonate dissolution or stable isotope fractionation to climatically induced changes. Hence, changes in root respiration and microbial activity due to changes in vegetation density seem to be responsible for increasing soil air δ^{13}C values probably due to lower soil respiration rates between 9 and 7 ka BP. This implies that the vegetation cover above the cave became thinner during this interval, which may be related to the relatively dry conditions between 7.7 to 7.3 ka BP inferred from the Mg/Ca ratio (Fig. 4a). After 6 ka, the stalagmite δ^{13}C signal decreases implying the development of a denser vegetation cover above the cave with concomitant higher soil bioproductivity.

Superimposed on this first-order trend in δ^{13}C, a higher frequency pattern is visible. This pattern resembles the second-order signal in Mg/Ca and is attributed to cave internal processes such as kinetic isotope fractionation. The degree of kinetic C isotope fractionation is mainly influenced by variations in drip rate (Dreybrodt, 2008; Mühlinghaus et al., 2009; Scholz et al., 2009; Deininger et al., 2012), which in turn reflects changes in karst hydrology and precipitation above the cave. Therefore, high

CPD
8, 1687–1720, 2012

δ^{13}C values are assigned to periods of low drip rates and vice versa. The overall similarity of the detrended and smoothed time series of Mg/Ca and δ^{13}C for Bu4 (Fig. 4a, b) implies that slow drip rates correspond to periods of less precipitation.

4.3 δ^{18}O values

Applying conventional evapo-transpiration equations, Wackerbarth et al. (2010) estimated that about 40–50 % of the annual precipitation is lost due to evapo-transpiration processes. Thus, the contribution of summer precipitation to recharge of the karst aquifer is very low in the cave region. Furthermore, Münsterer et al. (2012) demonstrated, based on analysis of ^{36}Cl, that the annual amount of evapo-transpiration is even higher and may reach values between 68 to 88 %. Thus, winter precipitation is the major proportion of the cave drip water and dominates its δ^{18}O value.

The relationship between surface air temperature variability and the stable oxygen isotope signal of precipitation are well understood (e.g. Lachniet, 2009). In general, lower temperatures should correspond to lower speleothem δ^{18}O values and vice versa. However, the δ^{18}O response of individual cave systems might differ. For example, for central Europe Wackerbarth et al. (2010) suggested that this positive relationship may not be valid when accounting for the positive relationship between the amount of winter precipitation and winter temperature. During warmer winters, the larger amount of precipitation contributing to the recharge water, which has generally lower δ^{18}O values than summer precipitation, leads to lower drip water δ^{18}O values. In total, higher winter temperatures (and higher mean annual temperatures) may, thus, result in lower δ^{18}O values for stalagmite calcite. In addition, in case of kinetic isotope fractionation, higher drip rates (probably due to increased precipitation) would also result in lower δ^{18}O values (Mühlinghaus et al., 2009; Scholz et al., 2009; Dreybrodt and Scholz, 2011; Deininger et al., 2012). Therefore, we interpret the observed variations in speleothem δ^{18}O as changes in both surface winter temperature and amount of winter

CPD
8, 1687–1720, 2012

precipitation. More positive $\delta^{18}O$ values reflect cold and dry winters, whereas more negative $\delta^{18}O$ values represent warmer and more humid winters.

The smoothed $\delta^{18}O$ record of Bu4 (21 point moving average) for the last 8 ka (Fig. 4c) shows large similarities with the detrended and smoothed Mg/Ca record (Fig. 4a). During relatively dry conditions (high Mg/Ca ratio), the $\delta^{18}O$ values show more positive values than during relatively humid conditions (low Mg/Ca ratio). This pattern is particularly pronounced between 7.8 and 7.3 ka, 6 and 5.5 ka, 2.8 and 2.2 ka and during the LIA. In contrast, this relationship of high Mg/Ca and high $\delta^{18}O$ does not hold for the period from 4.5 to 3.5 ka. As described above, changes in carbonate dissolution processes and PCP may be responsible for the observed variability in Mg/Ca. Variable PCP may also affect the $\delta^{18}O$ signal. However, for the Bunker Cave stalagmites, PCP seems not to be of major importance for the $\delta^{18}O$ values. This is confirmed by the differences in the Mg/Ca ratios of Bu1 and Bu4 (Fig. 3a). Bu1 only shows small variations in Mg/Ca indicating negligible PCP, but the $\delta^{18}O$ values are very similar to those of Bu4, which shows relatively large variations in Mg/Ca suggesting a strong influence of PCP. Furthermore, peaks in Mg/Ca are in most cases not coeval with peaks in $\delta^{18}O$, which provides additional evidence that PCP did not strongly influence the speleothem $\delta^{18}O$ values in Bunker Cave.

Data and modelling studies (Baldini et al., 2008; Langebroek et al., 2011) showed that $\delta^{18}O$ values in precipitation over central Western Europe are influenced by a North Atlantic Oscillation (NAO) like pattern. As argued in Langebroek et al. (2011), the correlation pattern between the $\delta^{18}O$ value of precipitation and atmospheric circulation over Europe is a result of the combined effect of temperature and precipitation. Heat and moisture are mainly transported to the European continent from the North Atlantic by the westerlies. Therefore, climatic-related signals from the North Atlantic (e.g. the hematite-stained grains (HSG) record; Bond et al., 2001) and the Bunker Cave $\delta^{18}O$ record are expected to show similar variations (Fig. 5). Cold periods as indicated by increased percentages of HSG indeed coincide in most cases with colder phases in Western Germany (high $\delta^{18}O$ values in speleothem calcite).

CPD
8, 1687–1720, 2012

Ostracod $\delta^{18}O$ values from Lake Ammersee (von Grafenstein et al., 1998, 1999) reflect the $\delta^{18}O$ value of precipitation (Fig. 5b) over the northern rim of the Alps and are here used to constrain the $\delta^{18}O$ value of soil water above Bunker Cave. The signal-to-noise ratio of the Ammersee data is comparable to that of the composite Bunker Cave $\delta^{18}O$ record (Fig. 5c). Throughout the Holocene, the composite $\delta^{18}O$ record of the four Bunker Cave stalagmites shows values ranging from −7 to −5 ‰ and broadly follows the precipitation $\delta^{18}O$ signal reconstructed from Lake Ammersee. However, the Bunker cave $\delta^{18}O$ data highlight longer periods of high or low $\delta^{18}O$ values whose amplitude is also larger than that of the Ammersee record, suggesting that processes in soil and cave may modify the $\delta^{18}O$ value of the rainfall preserved in the stalagmites. In particular, variations in the (degree of) kinetic isotope fractionation may have a strong influence.

When comparing the Bunker Cave $\delta^{18}O$ record with the $\delta^{18}O$ records from Atta Cave (Niggemann, 2000; Niggemann et al., 2003), Katerloch (Boch et al., 2009) and Spannagel Cave (Vollweiler et al., 2006), a similar structure is observed in all records. This indicates that the signal encoded in the Bunker Cave stalagmites represents supra-regional climate. A comparison of the composite Bunker Cave record and the other European stalagmite archives (Fig. 5) with the HSG record from the North Atlantic (Bond et al., 2001) suggests that the signal from the central European continent may even be representative for the North Atlantic region and large parts of Europe.

4.3.1 Little Ice Age vs. 8.2 ka event

Two prominent features in the composite Bunker Cave $\delta^{18}O$ record (Fig. 5c) are the 8.2 ka event and the Little Ice Age (LIA), which occurred between 0.7 to 0.2 ka BP. The LIA is characterized by high Mg/Ca ratios as well as prominent maxima in $\delta^{13}C$ and $\delta^{18}O$ in the Bunker record. The $\delta^{18}O$ values are the highest of the entire record. According to our interpretation, this shows that during the LIA, central Europe experienced anomalously cold and dry winter conditions in agreement with the cold conditions

CPD
8, 1687–1720, 2012

observed in the North Atlantic (Bond et al., 2001) and a pronounced negative anomaly of the NAO during this period (Trouet et al., 2009).

Another prominent Holocene cold event was the 8.2 ka event. This abrupt event brought generally cold and dry conditions to the Northern Hemisphere, in particular during winter (Alley et al., 1997; Alley and Ágústsdóttir, 2005). This event was triggered by large amounts of melt water originating from the North American continent that freshened the North Atlantic and influenced the North Atlantic circulation by a curtailment of North Atlantic Deep Water (NADW) formation (Alley et al., 1997; Barber et al., 1999; Rohling and Pälike, 2005). In Central-Northern Europe, this event led to more negative δ^{18}O values in precipitation (von Grafenstein et al., 1999; LeGrande and Schmidt, 2008). This depletion in rainfall δ^{18}O is also recorded in the Bunker Cave δ^{18}O record (Fig. 5). However, the amplitude of the 8.2 ka event in the stalagmite record is lower than in the Ammersee precipitation record. Furthermore, Mg/Ca ratios of the Bunker Cave record are relatively low during the 8.2 ka event (Fig. 4a) suggesting average or slightly more humid conditions. Thus, climate conditions were probably not exceptionally dry in central Europe during the 8.2 ka event.

5 Conclusions

A multi-proxy study of four Holocene speleothems from Bunker Cave is presented. The Mg/Ca ratio, δ^{13}C and δ^{18}O data allow a consistent reconstruction of past winter climate variability in central Europe. High Mg/Ca values in the detrended record depict dry periods within the Holocene. Accordingly, high δ^{13}C values of the detrended record are ascribed to low drip rates due to dry conditions above the cave. More positive δ^{18}O values during the last 10.8 ka reflect lower winter temperature and less winter rainfall. An exception in this context is the 8.2 ka cold event, which shows a prominent negative δ^{18}O excursion. This is ascribed to a negative anomaly in the δ^{18}O values of precipitation over central Europe triggered by changes in the North Atlantic Ocean circulation due to increased freshwater input. The δ^{18}O values from the Bunker Cave

CPD
8, 1687–1720, 2012

stalagmites agree well with other central European climate archives as well as with records from the North Atlantic. Cold and dry periods are observed between 9 and 7 ka, 6.5 and 5.5 ka, 4 and 3 ka as well as between 0.7 to 0.2 ka.

Acknowledgements. This work was funded by DFG research grant FG 668 (DAPHNE).

References

Alley, R. B. and Ágústsdóttir, A. M.: The 8k event: cause and consequences of a major Holocene abrupt climate change, Quaternary Sci. Rev., 24, 1123–1149, 2005. 1706

Alley, R. B., Mayewski, P. A., Sowers, T., Stuiver, M., Taylor, K. C., and Clark, P. U.: Holocene climatic instability: A prominent, widespread event 8200 yr ago, Geology, 25, 483–486, 1997. 1689, 1706

Baldini, J. U. L., McDermott, F., Hoffmann, D. L., Richards, D. A., and Clipson, N.: Very high-frequency and seasonal cave atmosphere pCO_2 variability: implications for stalagmite growth and oxygen isotope-based paleoclimate records, Earth Planet. Sci. Lett., 272, 118–129, 2008. 1704

Barber, D. C., Dyke, A., Hillaire-Marcel, C., Jennings, A. E., Andrews, J. T., Kerwin, M. W., Bilodeau, G., McNeely, R., Southon, J., Morehead, M. D., and Gagnon, J.-M.: Forcing of the cold event of 8200 yr ago by catastrophic drainage of Laurentide lakes, Nature, 400, 344–348, 1999. 1706

Boch, R., Spötl, C., and Kramers, J.: High-resolution isotope records of early Holocene rapid climate change from two coeval stalagmites of Katerloch Cave, Austria, Quaternary Sci. Rev., 28, 2527–2538, 2009. 1690, 1705, 1720

Bond, G., Kromer, B., Beer, J., Muscheler, R., Evans, M., Showers, W., Hoffmann, S., Lotti-Bond, R., Hajdas, I., and Bonani, G.: Persistent solar influence on North Atlantic climate during the Holocene, Science, 294, 2130–2136, 2001. 1704, 1705, 1706, 1720

Büntgen, U., Trouet, V., Frank, D., Leuschner, H. H., Friedrichs, D., Luterbacher, J., and Esper, J.: Tree-ring indicators of German summer drought over the last millennium, Quaternary Sci. Rev., 29, 1005–1016, 2010. 1690

Cheng, H., Edwards, R. L., Hoff, J., Gallup, C. D., Richards, D. A., and Asmerom, Y.: The half-lives of uranium-234 and thorium-230, Chem. Geol., 169, 17–33, 2000. 1692

CPD
8, 1687–1720, 2012

Cruz Jr, F. W., Burns, S. J., Jercinovic, M., Karmann, I., Sharp, W. D., and Vuille, M.: Evidence of rainfall variations in Southern Brazil from trace element ratios (Mg/Ca and Sr/Ca) in a rate Pleistocene stalagmite, Geochim. Cosmochim. Ac., 71, 2250–2263, 2007. 1699

Davis, B. A. S., Brewer, S., Stevenson, A. C., and Guiot, J.: The temperature of Europe during the Holocene reconstructed from pollen data, Quaternary Sci. Rev., 22, 1701–1716, 2003. 1690

Deininger, M., Fohlmeister, J., and Mangini, A.: The influence of evaporation effects on the carbon and oxygen isotope composition of speleothems – a model approach, Geochim. Cosmochim. Ac., submitted, 2012. 1702, 1703

Dreybrodt, W.: Evolution of isotopic composition of carbon and oxygen in a calcite precipitating H_2O-CO_2-$CaCO_3$ solution and the related isotopic composition of calcite in stalagmites, Geochim. Cosmochim. Ac., 72, 4712–4724, 2008. 1702

Dreybrodt, W. and Scholz, D.: Climatic dependence of stable carbon and oxygen isotope signals recorded in speleothems: From soil water to speleothem calcite, Geochim. Cosmochim. Ac., 75, 734–752, 2011. 1701, 1703

Fairchild, I. J. and Treble, P. C.: Trace elements in speleothems as recorders of environmental change, Quaternary Sci. Rev., 28, 449–468, 2009. 1698, 1700

Fohlmeister, J.: A statistical approach to construct composite climate records of dated archives, Quat. Geochronol., submitted, 2012. 1696, 1697, 1717

Fohlmeister, J., Kromer, B., and Mangini, A.: The influence of soil organic matter age spectrum on the reconstruction of atmospheric ^{14}C levels via stalagmites, Radiocarbon, 53, 99–115, 2011. 1695

Frank, N., Braum, M., Hambach, U., Mangini, A., and Wagner, G.: Warm period growth of travertine during the last interglaciation in Southern Germany, Quaternary Res., 54, 38–48, 2000. 1692

Friedrich, M., Kromer, B., Spurk, M., Hofmann, J., and Kaiser, K. F.: Paleo-environment and radiocarbon calibration as derived from lateglacial/early Holocene tree-ring chronologies, Quatern. Int., 61, 27–39, 1999. 1690

Frisia, S. and Borsato, A.: Karst, Devel. Sedimentol., 61, 269–318, 2010. 1700

Frisia, S., Borsato, A., Preto, N., and McDermott, F.: Late Holocene annual growth in three alpine stalagmites records the influence of solar activity and the North Atlantic oscillation on winter climate, Earth Planet. Sci. Lett., 216, 411–424, 2003. 1690

CPD
8, 1687–1720, 2012

Frisia, S., Fairchild, I. J., Fohlmeister, J., Miorandi, R., Spötl, C., and Borsato, A.: Carbon mass-balance modelling and carbon isotope exchange processes in dynamic caves, Geochim. Cosmochim. Ac., 75, 380–400, 2011. 1701, 1702

Genty, D. and Massault, M.: Carbon transfer dynamics from bomb-^{14}C and δ^{13}C time series of a laminated stalagmite from SW France – modeling and comparison with other stalagmite records, Geochim. Cosmochim. Ac., 63, 1537–1548, 1999. 1695

Gerdes, A. and Zeh, A.: Combined U-Pb and Hf isotope LA-(MC-)ICP-MS analyses of detrital zircons: comparison with SHRIMP and new constraints for the provenance and age of an armorican metasediment in Central Germany, Earth Planet. Sci. Lett., 249, 41–67, 2006. 1693

Griffiths, M. L., Fohlmeister, J., Drysdale, R. N., Hua, Q., Johnson, K. R., Hellstrom, J. C., Gagan, M. K., and Zhao, J.-X.: Hydrological control on the dead-carbon content of a Holocene tropical speleothem, Quat. Geochronol., in press, doi:10.1016/j.quageo.2012.04.001, 2012. 1701

Guiot, J., Harrison, S. P., and Prentice, I. C.: Reconstruction of Holocene precipitation patterns in Europe using pollen and lake-level data, Quaternary Res., 40, 139–149, 1993. 1690

Hammerschmidt, E., Niggemann, S., Grebe, W., Oelze, R., Brix, M. R., and Richter, D. K.: Höhlen in Iserlohn, Schr. Karst. Höhlenkd. Westf., 1, 1–154, 1995. 1699

Hill, C. and Forti, P.: Cave minerals of the world, Vol. 2, National speleological society, Huntsville, AL, 1997. 1700

Hoffmann, D. L., Prytulak, J., Richards, D. A., Elliott, T., Coath, C. D., Smart, P. L., and Scholz, D.: Procedures for accurate U and Th isotope measurements by high precision MC-ICPMS, Int. J. Mass Spectrom., 264, 97–109, 2007. 1692

Holzhauser, H., Magny, M., and Zumbühl, H. J.: Glacier and lake-level variations in West-Central Europe over the last 3500 yr, Holocene, 15, 789–801, 2005. 1690

Holzkämper, S., Spötl, C., and Mangini, A.: High-precision constraints on timing of alpine warm periods during the middle to late Pleistocene using speleothem growth periods, Earth Planet. Sci. Lett., 236, 751–764, 2005. 1692

Hua, Q. and Barbetti, M.: Review of tropospheric bomb ^{14}C data for carbon cycle modeling and age calibration purposes, Radiocarbon, 46, 1273–1298, 2004. 1695

Immenhauser, A., Buhl, D., Richter, D. K., Niedermayr, A., Riechelmann, D. F. C., Dietzel, M., and Schulte, U.: Magnesium-isotope fractionation during low-Mg calcite precipitation in a

CPD
8, 1687–1720, 2012

limestone cave – field study and experiments, Geochim. Cosmochim. Ac., 74, 4346–4364, 2010. 1691
Ivy-Ochs, S., Kerschner, H., Maisch, M., Christl, M., Kubik, P. W., and Schlüchter, C.: Latest Pleistocene and Holocene glacier variations in the European Alps, Quaternary Sci. Rev., 28, 2137–2149, 2009. 1690
Joerin, U. E., Stocker, T. F., and Schlüchter, C.: Multicentury glacier fluctuations in the Swiss Alps during the Holocene, Holocene, 16, 697–704, 2006. 1690
Kluge, T., Riechelmann, D. F. C., Wieser, M., Spötl, C., Sültenfuß, J., Schröder-Ritzrau, A., Niggemann, S., and Aeschbach-Hertig, W.: Dating cave drip water by tritium, J. Hydrol., 349, 396–406, 2010. 1691
Lachniet, M. S.: Climatic and environmental controls on speleothem oxygen-isotope values, Quaternary Sci. Rev., 28, 412–432, 2009. 1703
Langebroek, P. M., Werner, M., and Lohmann, G.: Climate information imprinted in oxygen-isotopic composition of precipitation in Europe, Earth Planet. Sci. Lett., 311, 144–154, 2011. 1704
LeGrande, A. N. and Schmidt, G. A.: Ensemble, water isotope-enabled, coupled general circulation modeling insights into the 8.2 ka event, Paleoceanography, 23, PA3207, doi:10.1029/2008PA001610, 2008. 1706
Levin, I. and Kromer, B.: The tropospheric $^{14}CO_2$ level in mid-latitudes of the Northern Hemisphere (1959–2003), Radiocarbon, 46, 1261–1272, 2004. 1695
Magny, M.: Holocene climate variability as reflected by mid-European lake-level fluctuations and its probable impact on prehistoric human settlements, Quatern. Int., 113, 65–79, 2004. 1690
Mangini, A., Spötl, C., and Verdes, P.: Reconstruction of temperature in the Central Alps during the past 2000 yr from a $\delta^{18}O$ stalagmite record, Earth Planet. Sci. Lett., 235, 741–751, 2005. 1690
Mattey, D., Lowry, D., Duffet, J., Fisher, R., Hodge, E., and Frisia, S.: A 53 yr seasonally resolved oxygen and carbon isotope record from a modern Gibraltar speleothem: reconstructed drip water and relationship to local precipitation, Earth Planet. Sci. Lett., 269, 80–95, 2008. 1695
McDermott, F., Frisia, S., Huang, Y., Longinelli, A., Spiro, B., Heaton, T. H. E., Hawkesworth, C. J., Borsato, A., Keppens, E., Fairchild, I. J., van der Borg, K., Verheyden, S., and Selmo, E. M.: Holocene climate variability in Europe: evidence from $\delta^{18}O$, textural and

CPD
8, 1687–1720, 2012

extension-rate variations in three speleothems, Quaternary Sci. Rev., 18, 1021–1038, 1999. 1690

Mühlinghaus, C., Scholz, D., and Mangini, A.: Modelling fractionation of stable isotopes in stalagmites, Geochim. Cosmochim. Ac., 71, 2780–2790, 2009. 1702, 1703

Münsterer, C., Fohlmeister, J., Wackerbarth, A., Christl, M., Schröder-Ritzrau, A., Alfimov, V., Ivy-Ochs, S., and Mangini, A.: Cosmogenic ^{36}Cl in karst waters from Bunker Cave, North Western Germany – a tool to derive local evapotranspiration?, Geochim. Cosmochim. Ac., 86, 138–149, doi:10.1016/j.gca.2012.03.008, 2012. 1691, 1703

Neuser, R. D., Bruhn, F., Götze, J., Habermann, D., and Richter, D. K.: Kathodolumineszenz: Methodik und Anwendung, Zbl. Geo. Pal., 1/2, 287–306, 1995. 1694

Niggemann, S.: Klimabezogene Untersuchung an spät- und postglazialen Stalagmiten aus Massenkalkhöhlen des Sauerlandes, in: Beiträge zur Speläologie I, edited by: Richter, D. K. and Wurth, G., Bochumer geologische und geotechnische Arbeiten, Ruhr-University Bochum, Bochum, 5–129, 2000. 1705, 1720

Niggemann, S., Mangini, A., Mudelsee, M., Richter, D. K., and Wurth, G.: Sub-Milankovitch climatic cycles in Holocene stalagmites from Sauerland, Germany, Earth Planet. Sci. Lett., 216, 539–547, 2003. 1690, 1705, 1720

North Greenland Ice Core Project members: High-resolution record of Northern Hemisphere climate extending into the last interglacial period, Nature, 431, 147–151, 2004. 1690

Pearce, N. J. G., Perkins, W. T., Westgate, J. A., Gorton, M. P., Jackson, S. E., Neal, C. N., and Chenery, S.: A compilation of new and published major and trace element data for NIST SRM 610 and NIST SRM 612 glass reference material, Geostandard Newslett., 21, 115–144, 1996. 1694

Richter, D., Gotte, T., Niggemann, S., and Wurth, G.: REE3+ and Mn2+ activated cathodoluminescence in lateglacial and Holocene stalagmites of Central Europe: evidence for climatic processes?, Holocene, 14, 759–768, 2004. 1699

Riechelmann, D. F. C., Schröder-Ritzrau, A., Scholz, D., Fohlmeister, J., Spötl, C., Richter, D. K., and Mangini, A.: Monitoring of the Bunker Cave (NW Germany): assessing the complexity of cave environmental parameters, J. Hydrol., 409, 682–695, 2011. 1691, 1692, 1698, 1699, 1700

Riechelmann, D. F. C., Deininger, M., Scholz, D., Riechelmann, S., Schröder-Ritzrau, A., Spötl, C., Richter, D. K., Immenhauser, A., and Mangini, A.: Disequilibrium carbon and oxy-

CPD
8, 1687–1720, 2012

gen isotope fractionation in recent cave calcite: comparison of cave precipitates and numerical model $\delta^{13}C$ and $\delta^{18}O$ data, Geochim. Cosmochim. Ac., submitted, 2012. 1701
Riechelmann, S., Buhl, D., Schröder-Ritzrau, A., Spötl, C., Riechelmann, D. F. C., Richter, D. K., Kluge, T., Marx, T., and Immenhauser, A.: Hydrogeochemistry and fractionation pathways of Mg isotopes in a continental weathering system: Lessons from field experiments, Chem. Geol., 300, 109–122, 2012. 1699, 1700
Rohling, E. J. and Pälike, H.: Centennial-scale climate cooling with a sudden cold event around 8200 yr ago, Nature, 434, 975–979, 2005. 1706
Scholz, D. and Hoffmann, D.: StalAge – an algorithm designed for construction of speleothem age models, Quat. Geochronol., 6, 369–382, 2011. 1720
Scholz, D., Mühlinghaus, C., and Mangini, A.: Modelling $\delta^{13}C$ and $\delta^{18}O$ in the solution layer on stalagmite surfaces, Geochim. Cosmochim. Ac., 73, 2592–2602, 2009. 1701, 1702, 1703
Spötl, C. and Mattey, D.: Stable isotope microsampling of speleothems for palaeoenvironmental studies: a comparison of microdrill, micromill and laser ablation techniques, Chem. Geol., 235, 48–58, 2006. 1693
Spötl, C., Faichild, I. J., and Tooth, A. F.: Cave air control on dripwater geochemistry, Obir Cave (Austria): implications for speleothem deposition in dynamically ventilated caves, Geochim. Cosmochim. Ac., 69, 2451–2468, 2005. 1701
Spurk, M., Leuschner, H. H., Baillie, M. G. L., Briffa, K. R., and Friedrich, M.: Depositional frequency of German subfossil oaks: climatically and non-climatically induced fluctuations in the Holocene, Holocene, 12, 707–715, 2002. 1690
Synal, H.-A., Stocker, M., and Suter, M.: MICADAS: a new compact radiocarbon AMS system, Nucl. Instrum. Meth. B, 259, 7–13, 2007. 1693
Tooth, A. F. and Fairchild, I. J.: Soil and karst aquifer hydrological controls on the geochemical evolution of speleothem-forming drip waters, Crag Cave, Southwest Ireland, J. Hydrol., 273, 51–68, 2003. 1699
Tremaine, D. M., Froelich, P. N., and Wang, Y.: Speleothem calcite farmed in situ: modern calibration of $\delta^{18}O$ and $\delta^{13}C$ paleoclimate proxies in a continuously-monitored natural cave system, Geochim. Cosmochim. Ac., 75, 4929–4950, 2011. 1701
Trouet, V., Esper, J., Graham, N. E., Baker, A., Scourse, J. D., and Frank, D. C.: Persistent positive North Atlantic Oscillation mode dominated the medieval climate anomaly, Science, 324, 78–80, 2009. 1706

CPD
8, 1687–1720, 2012

Vollweiler, N., Scholz, D., Mühlinghaus, C., Mangini, A., and Spötl, C.: A precisely dated climate record for the last 9 kyr from three high alpine stalagmites, Spannagel Cave, Austria, Geophys. Res. Lett., 33, L20703, doi:10.1029/2006GL027662, 2006. 1690, 1705, 1720

von Grafenstein, U., Erlenkeuser, H., Müller, J., Jouzel, J., and Johnsen, S.: The cold event 8200 yr ago documented in oxygen isotope records of precipitation in Europe and Greenland, Clim. Dynam., 14, 73–81, 1998. 1689, 1705, 1720

von Grafenstein, U., Erlenkeuser, H., Brauer, A., Jouzel, J., and Johnsen, S. J.: A mid-European decadal isotope-climate record from 15 500 to 5000 yr BP, Science, 284, 1654–1657, 1999. 1705, 1706, 1720

Wackerbarth, A., Scholz, D., Fohlmeister, J., and Mangini, A.: Modelling the $\delta^{18}O$ value of cave drip water and speleothem calcite, Earth Planet. Sci. Lett., 299, 387–397, 2010. 1690, 1692, 1703

Wanner, H., Beer, J., Bütikofer, J., Crowley, T., Cubasch, U., Flückiger, J., Goosse, H., Grosjean, M., Joos, F., Kaplan, J., Küttel, M., Müller, S. A., Prentice, I. C., Solomina, O., Stocker, T. F., Tarasov, P., Wagner, M., and Widmann, M.: Mid-to late Holocene climate change: an overview, Quaternary Sci. Rev., 27, 1791–1828, 2008. 1690

Wanner, H., Solomina, O., Grosjean, M., Ritz, S. P., and Jetel, M.: Structure and origin of Holocene cold events, Quaternary Sci. Rev., 30, 310–3123, 2011. 1690

Wurth, G.: Klimagesteuerte Rhythmik in spät-bis postglazialen Stalagmiten des Sauerlandes, der Fränkischen Alb und der Bayerischen Alpen, Ph.D. thesis, Ruhr-Universität Bochum, Universitätsbibliothek, Bochum, 2002. 1701

CPD
8, 1687–1720, 2012

Table 1. Uranium and thorium isotopic compositions and ^{230}Th ages for Bunker Cave stalagmites Bu1, Bu2, Bu4 and Bu6 measured by TIMS. Errors are 2σ analytical errors. Corrected ^{230}Th ages assume an initial ^{230}Th/^{232}Th concentration ratio of 3.8 ± 1.9.

Sample ID	^{238}U [ppb]	^{232}Th [ppt]	δ^{234}U [‰]	(^{230}Th/^{238}U) act. ratio	age$_{uncorrected}$ [ka BP]	age$_{corrected}$ [ka BP]
Bu1						
Bu1 – 2 cm	44.4 ± 0.1	36 ± 2	390 ± 11	0.0078 ± 0.0027	0.57 ± 0.21	0.56 ± 0.21
Bu1 – 3.3 cm*	48.08 ± 0.1	274 ± 29	354 ± 10	0.0082 ± 0.0023	0.72 ± 0.18	0.60 ± 0.20
Bu1 – 9 cm	58.5 ± 0.1	57 ± 1	332 ± 8	0.0139 ± 0.0017	1.11 ± 0.14	1.09 ± 0.14
Bu1 – 14 cm	39.8 ± 0.1	74 ± 1	336 ± 8	0.0193 ± 0.0019	1.57 ± 0.16	1.53 ± 0.16
Bu1 – 31 cm	61.5 ± 0.1	1004 ± 8	292 ± 4	0.0547 ± 0.0052	5.02 ± 0.46	4.66 ± 0.48
Bu1 – 35 cm	60.4 ± 0.1	1403 ± 8	283 ± 5	0.0581 ± 0.0014	5.50 ± 0.13	4.98 ± 0.30
Bu1 – 39.5 cm	68.6 ± 0.1	661 ± 4	252 ± 9	0.0653 ± 0.0026	6.00 ± 0.25	5.78 ± 0.28
Bu1 – 42 cm	84.6 ± 0.1	1317 ± 6	287 ± 4	0.0737 ± 0.0025	6.70 ± 0.23	6.36 ± 0.29
Bu1 – 46 cm	90.7 ± 0.2	100 ± 1	278 ± 6	0.0735 ± 0.0017	6.42 ± 0.16	6.40 ± 0.15
Bu1 – 49 cm	120.6 ± 0.1	891 ± 8	271 ± 6	0.0759 ± 0.0065	6.81 ± 0.59	6.64 ± 0.59
Bu2						
Bu2 – 1 cm	57.1 ± 0.1	2099 ± 19	440 ±9	0.0989 ± 0.0029	8.39 ± 0.25	7.66 ± 0.46
Bu2 – 4 cm	116.6 ± 0.2	221 ± 3	437 ± 7	0.1174 ± 0.0033	9.24 ± 0.27	9.20 ± 0.27
Bu2 – 5.5 cm	135.9 ± 0.1	597 ± 3	442 ± 5	0.1288 ± 0.0021	10.20 ± 0.18	10.11 ± 0.18
Bu2 – 7 cm	191.6 ± 0.2	304 ± 2	564 ± 4	0.1469 ± 0.0025	10.68 ± 0.19	10.65 ± 0.19
Bu4						
Bu4 – 1.45 cm*	66 ± 0.1	54 ± 33	662 ± 24	0.0135 ± 0.0022	0.85 ± 0.15	0.83 ± 0.15
Bu4 – 3 cm	79.5 ± 0.2	47 ± 0	501 ± 7	0.0157 ± 0.0019	1.10 ± 0.14	1.09 ± 0.14
Bu4 – 5.5 cm	75.4 ± 0.2	1881 ± 9	514 ± 7	0.0204 ± 0.0011	1.89 ± 0.08	1.42 ± 0.26
Bu4 – 7 cm	72.0 ± 0.1	590 ±4	548 ± 7	0.0256 ± 0.0020	1.91 ± 0.14	1.76 ± 0.16
Bu4 – 9 cm	68.6 ± 0.1	227 ± 2	582 ± 8	0.0361 ± 0.0018	2.52 ± 0.13	2.46 ± 0.13
Bu4 – 10.15 cm*	57.7 ± 0.1	592 ± 31	558 ± 10	0.0480 ± 0.0022	3.53 ± 0.16	3.35 ± 0.19
Bu4 – 12 cm	95.8 ± 0.2	390 ± 2	598 ± 7	0.0569 ± 0.0021	3.96 ± 0.15	3.89 ± 0.16
Bu4 – 13.6 cm*	102.9 ± 0.2	1038 ± 27	587 ± 7	0.0724 ± 0.0016	5.20 ± 0.11	5.02 ± 0.15
Bu4 – 15.1 cm*	69.1 ± 0.1	2019 ± 27	664 ± 7	0.0888 ± 0.0034	6.39 ± 0.24	5.89 ± 0.36
Bu4 – 17.1 cm*	69 ± 0.1	1200 ± 41	600 ± 10	0.1027 ± 0.0051	7.45 ± 0.37	7.14 ± 0.41
Bu4 – 19.25 cm*	84.1 ± 0.2	368 ± 30	537 ± 9	0.1103 ± 0.0029	8.11 ± 0.22	8.03 ± 0.23
Bu6						
Bu6 – 0.8 cm	219.1 ± 0.4	1437 ± 8	277 ± 4	0.0996 ± 0.0017	8.93 ± 0.16	8.78 ± 0.18
Bu6 – 2.5 cm	199.4 ± 0.4	333 ± 2	271 ± 5	0.1127 ± 0.0018	10.08 ± 0.18	10.04 ± 0.18
Bu6 – 3.8 cm	237.0 ± 0.5	2779 ± 14	275 ± 6	0.1190 ± 0.0032	10.86 ± 0.30	10.59 ± 0.34

* Samples marked by an asterisk indicate addition of extra Th (see Sect. 2.2).

CPD
8, 1687–1720, 2012

Table 2. ^{14}C activity of the top sections from stalagmites Bu1 and Bu4.

sample name	depth [mm]	HD analysis number	^{14}C activity [pm C]	1σ error [pm C]
Bu1 xix	0.1 ± 0.1	29116	91.35	0.25
Bu1 xx	0.5 ± 0.3	29117	91.81	0.24
Bu1 x	1.0 ± 0.5	26607	91.14	0.25
Bu4 Top	0.05 ± 0.05	28403	97.44	0.27
Bu4 1 mm	0.6 ± 0.5	28404	100.15	0.26
Bu4 2 mm	1.6 ± 0.5	28405	87.83	0.23

CPD
8, 1687–1720, 2012

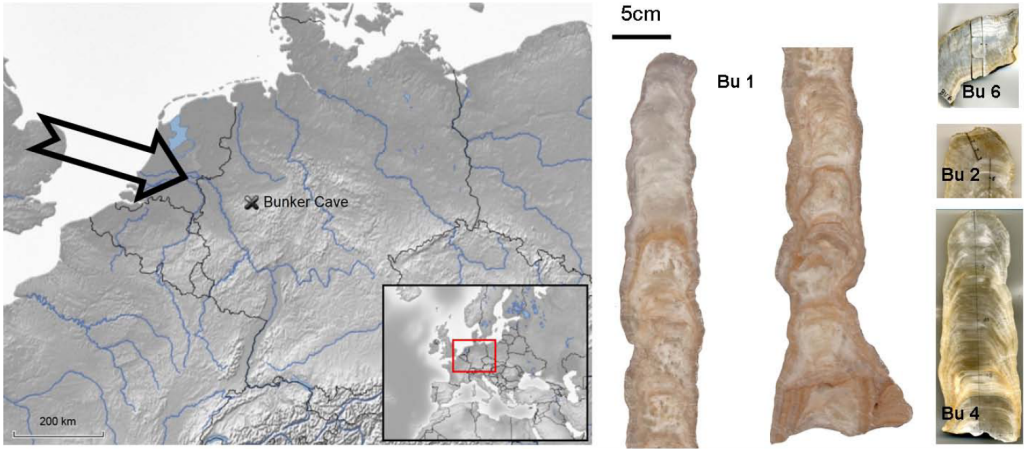

Fig. 1. Map of Central Europe showing the location of Bunker Cave. Central Europe is strongly influenced by the westerly wind system (indicated by the black solid arrow). The four studied stalagmites from Bunker cave are shown on the right. For Bu2, only the Holocene part of the sample is shown.

CPD
8, 1687–1720, 2012

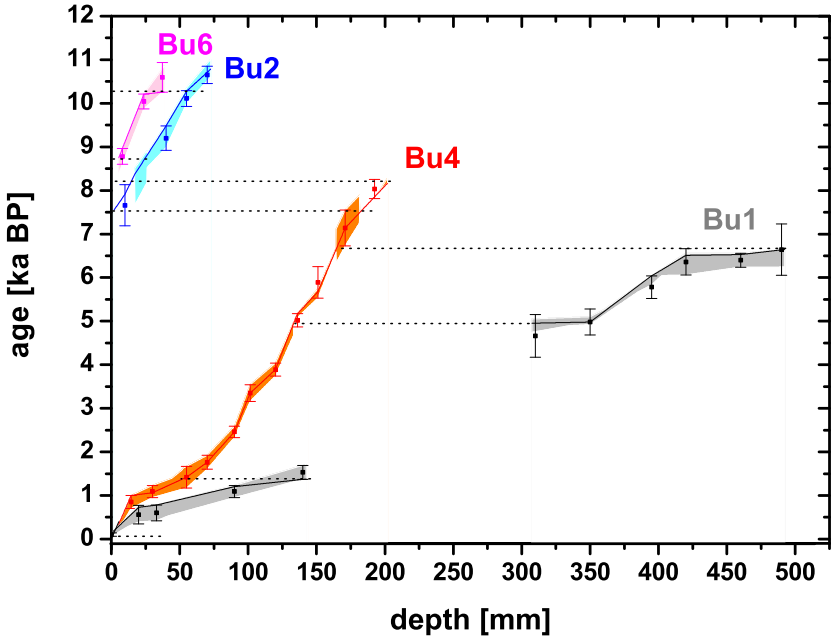

Fig. 2. Th/U ages (solid squares) and associated 2σ-uncertainties as well as the age-depth models (solid line) for the four stalagmites calculated using *iscam* (Fohlmeister, 2012).The shaded areas define the 2σ-uncertainty range. The thin dotted lines denote periods that are contained in two stalagmites (i.e. overlapping sections).

CPD
8, 1687–1720, 2012

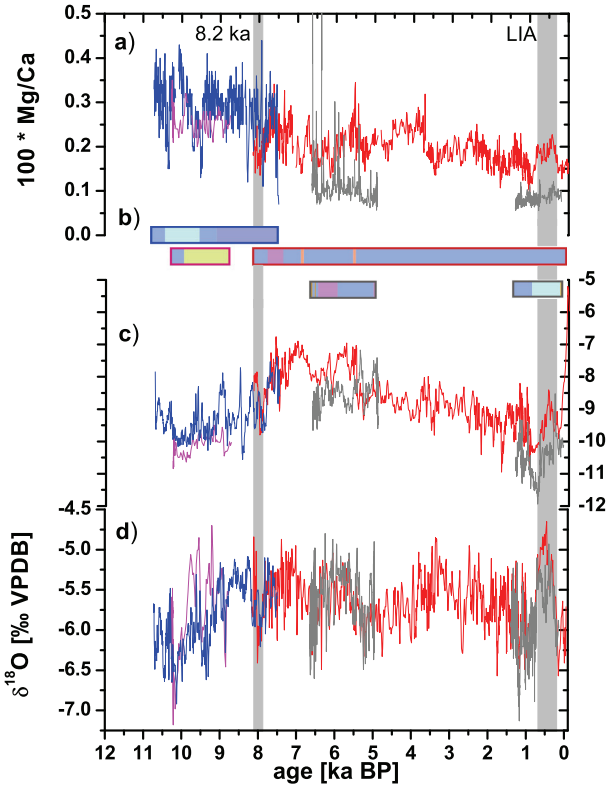

Fig. 3. Time series of 100*Mg/Ca **(a)**, petrographic logs **(b)**, $\delta^{13}C$ **(c)** and $\delta^{18}O$ **(d)** for Bu1 (grey), Bu4 (red), Bu2 (blue) and Bu6 (magenta). The vertical light grey lines represent large-scale European cold events (i.e. the 8.2 ka event, 8.2 ka, and the Little Ice Age, LIA). Colour code for the different fabrics are: blue: columnar; grey: elongated columnar; aqua: short columnar; yellow: open columnar; pink: dendritic; orange: coralloids and/or detrital layers.

CPD
8, 1687–1720, 2012

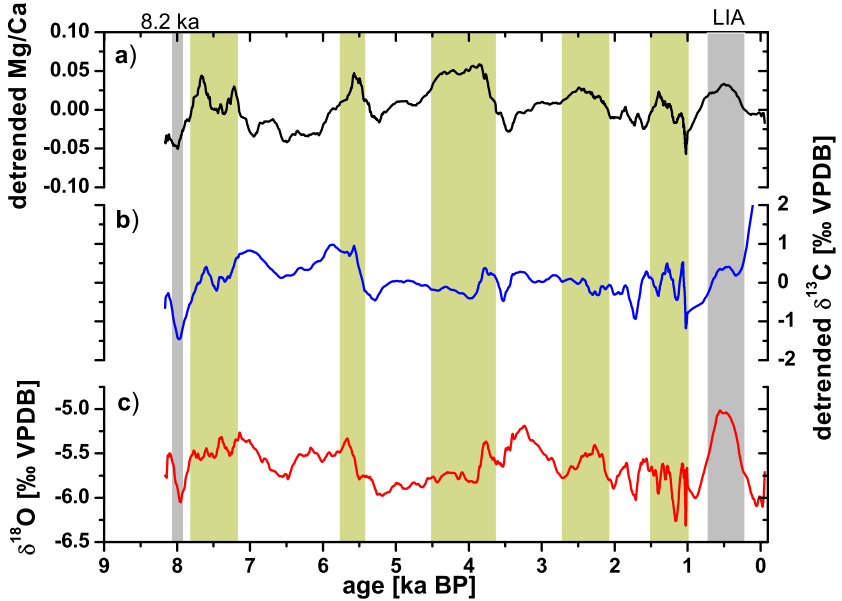

Fig. 4. Comparison of the detrended and smoothed (21 point moving average) Mg/Ca ratio **(a)** and δ^{13}C record **(b)** with the smoothed (21 point moving average) δ^{18}O record **(c)** of Bu4. The vertical light grey boxes represent the 8.2 ka event and the LIA. The yellow boxes represent periods of below average precipitation as indicated by elevated Mg/Ca ratios.

CPD
8, 1687–1720, 2012

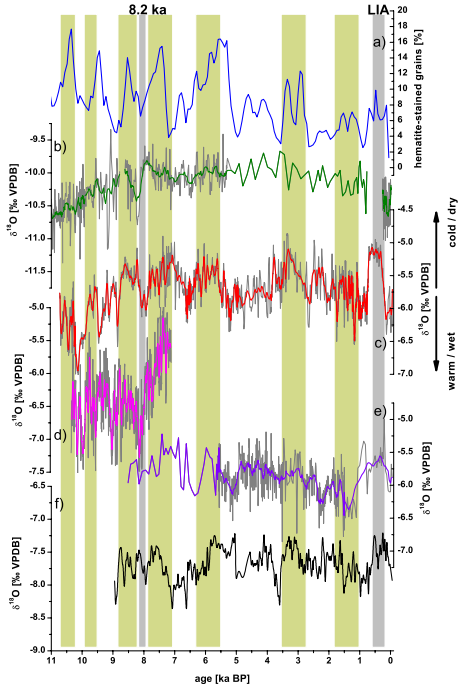

Fig. 5. **(c)** Composite δ^{18}O record from Bunker Cave in comparison to **(a)** hematite-stained grains from the North Atlantic (Bond et al., 2001), **(b)** Lake Ammersee (about 550 km south-east of Bunker Cave) a proxy of δ^{18}O of meteoric precipitation (von Grafenstein et al., 1998, 1999), **(d)** δ^{18}O record from Katerloch (Boch et al., 2009), **(e)** δ^{18}O record from stalagmite AH1 (Niggemann, 2000; Niggemann et al., 2003) from the Atta Cave (about 50 km south of Bunker Cave) and **(f)** the δ^{18}O record from the Austrian Alps (COMNISPA, Vollweiler et al., 2006). Thin grey lines represent the original data, which were smoothed with an 11-point moving average (coloured thick lines). The Ammersee data between 5.35 and 0.8 ka and the AH1 data between 8.5 and 6 ka BP are not smoothed due to their low temporal resolution. The AH1 data are shown on a new age-scale calculated with *StalAge* (Scholz and Hoffmann, 2011).

CPD
8, 1687–1720, 2012